Efficiency Measurement Techniques for Calibration of a Prototype 34-Meter-Diameter Beam-Waveguide Antenna at 8.45 and 32 GHz

Stephen D. Slobin, Tom Y. Otoshi, *Senior Member, IEEE,* Michael J. Britcliffe, Leon S. Alvarez, *Member, IEEE,* Scott R. Stewart, *Member, IEEE,* and Manuel M. Franco, *Member, IEEE*

***Abstract*—Efficiency measurements at 8.45 and 32 GHz (*X*- and *Ka*-bands) have been carried out on a new 34-meter-diameter beam-waveguide antenna now in use at the NASA/JPL Goldstone Deep Space Communications Complex. The use of portable test packages enabled measurements at both the Cassegrain and beam-waveguide focal points. Radio sources (quasars and Venus) were used as calibrators, and updated determinations of flux and source size correction were made during the period of the measurements. Gain and efficiency determinations as a function of elevation angle are presented, and the effects of the beam-waveguide system and antenna structure are clearly seen. At the beam-waveguide focus, an 8.45-GHz peak efficiency of 72.38 percent was measured; at 32 GHz, 44.89 percent was measured.**

I. Introduction

FROM July 1990 through January 1991, a new 34-meter-diameter beam-waveguide (BWG) antenna at the NASA/JPL Goldstone Deep Space Communications Complex in the Mojave Desert was tested as part of its post-construction performance evaluation. This antenna (designated "DSS 13 BWG") is the prototype for a new generation of Deep Space Network (DSN) antennas utilizing the BWG-type of antenna feed system. Fig. 1 shows a photograph of the new antenna. The mechanical design and focal points of the antenna may be found in Fig. 2 of a companion article [1].

Efficiency and pointing performance were characterized at 8.45 and 32 GHz (*X*- and *Ka*-bands, respectively) at both the Cassegrain (f1) and BWG (f3) focal points. The f1 focal point is located close to the vertex of the main reflector, while the f3 focal point is located about 35 meters and six additional reflectors distant in a subterranean pedestal room. The BWG type of design enables the simultaneous use of numerous different feeds in the relatively well-controlled conditions of the pedestal room, as contrasted with the present DSN situation of feedhorns, waveguide components, and low-noise amplifiers all installed above the surface of the dish where maintenance and modification tasks are considerably more difficult. In addition, increased system noise temperature due to rain on the feedhorn covers and dichroic plates is eliminated.

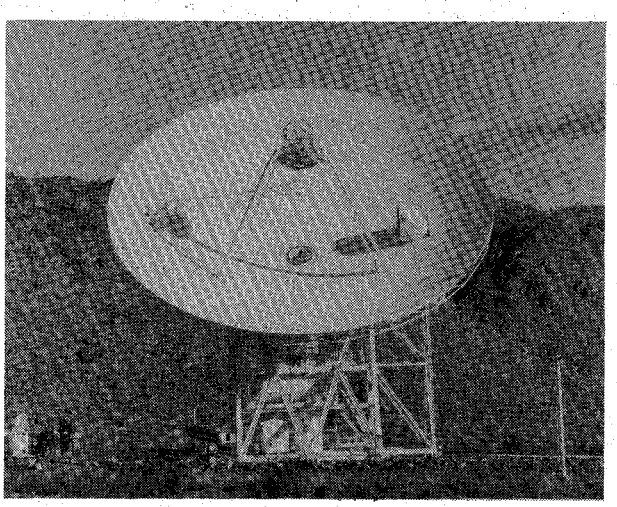

Fig. 1. Photograph of the NASA/JPL DSN beam-waveguide antenna at Goldstone, DSS 13.

The performance evaluation methods described in this article are unique in that a direct experimental measurement was made of the antenna efficiency and gain degradation caused by the BWG mirror system. The tests involved the use of *X*- and *Ka*-band portable test packages that were installed at either focal point f1 or f3.

To the authors' knowledge, this is the first known use of portable test packages to determine gain and efficiency at various locations in the microwave optics path of an antenna (see also [2], this issue).

Section II of this article presents the boresight measurement technique and pointing correction methodology used in looking at calibration radio sources of both known and unknown flux and source size correction values. Section III describes the methodology of antenna efficiency determination. Section IV presents methods for atmospheric attenuation correction. Section V presents characteristics of the radio sources used during the boresight

Manuscript received May 30, 1991; revised October 11, 1991. The research described in this paper was carried out by the Jet Propulsion Laboratory, California Institute of Technology, under a contract with the National Aeronautics and Space Administration.

The authors are with the Jet Propulsion Laboratory, California Institute of Technology, 4800 Oak Grove Drive, Pasadena, CA 91109.

IEEE Log Number 9107475.

measurements. The last sections present the results of the measurements and final deduced values of flux and source size correction for the not-well-known calibration radio sources.

II. Boresight Technique

Critical to the proper performance of the measurements was the use of a boresighting procedure to accurately point the antenna at the radio sources used in the calibration process. The method used was a seven-point boresight technique. This method moved the antenna sequentially in both the cross-elevation (XEL) and elevation (EL) directions both on and off the source. In each direction, the antenna was positioned off source ten half-power (one-sided) beamwidths, one half-power beamwidth at the so-called "3-dB" point, approximately 0.576 half-power beamwidths at the "1-dB" point, on source, and then similar offsets on the other side. For example, at *X*-band with the 34-meter antenna, the full 3-dB beamwidth is 65 mdeg. The offsets used were 325, 32.5, 18.7, and 0 mdeg in each direction. At *Ka*-band with a full 3-dB beamwidth of 17 mdeg, the offsets were 85, 8.5, 4.9, and 0 mdeg. For each scan, an off-source baseline is generated from the two off-source points. A gaussian curve (relative to the baseline) is fitted to the five remaining "on-source" points and the peak value of the curve is calculated. Also, the position of the peak is calculated as a measure of the pointing error for that scan. One pair of scans (one XEL and one EL) is considered to be one measurement or data point. The seven pointing offsets for each new scan are corrected for pointing errors found from the previous similar scan, so as to maintain pointing throughout a track. As an example, if for a particular a priori pointing software model installed in the ACS (antenna control subsystem) it is found that from boresight-to-boresight a consistent +3 mdeg pointing error is found in the elevation scans, this correction is made for each subsequent scan so as to maintain accurate pointing. After 10 boresights a 30-mdeg total pointing error relative to the original model will have been found, although the individual scan-to-scan pointing error will not exceed 3 mdeg. For the purposes of the efficiency measurements, it is thus assumed that perfect pointing is maintained for all scans and that the small calculated pointing errors are due to random errors in the system noise temperature measurements, rather than due to actual mis-pointing. No efficiency corrections for any small pointing errors were made in these measurements. Data points that were obviously bad were discarded.

Two data files are generated during the measurements—an efficiency file and a pointing file. The efficiency file consists of time, azimuth, elevation, and XEL and EL estimates of half-power beamwidth, peak source noise temperature contribution, and scan pointing error. The pointing file consists of time, azimuth, elevation, and pointing correction. Pointing correction is a cumulative value calculated from the sum of the pointing errors determined from the previous boresights. For example, if the first three boresights found +3, +2, and +4 mdeg pointing errors (relative to the a priori pointing model) in the elevation scans, the total accumulated pointing correction needed after the third boresight would be −9 mdeg. This correction is used in the generation of a new systematic pointing error correction model for use in future measurements. With a perfect pointing error correction model, the scan-to-scan pointing errors would be small and of random sign.

This boresight technique was developed at the Jet Propulsion Laboratory into a computer-assisted interactive program (named "Autobore") utilizing simultaneous operation of a personal computer and the antenna LCD (local control and display) console for pointing the antenna, determining and entering pointing offsets, entering noise temperature data, calculating radio source peak noise contribution, and determining antenna pointing errors.

III. Antenna Efficiency Determination

For a radio source of known flux density, the increase in system noise temperature as determined by the boresight measurements is a measure of the antenna efficiency. As defined here, the efficiency is referred to the input of the low-noise amplifier (cooled HEMT) and includes the losses of the feed system. Alternative methods specify efficiency at the aperture of the feedhorn or at the antenna aperture itself. The term "aperture efficiency" refers to antenna gain relative to that of a uniformly illuminated circular aperture having the same diameter as the antenna, e.g., a 70-percent efficient antenna has 1.549 dB less peak gain than does the circular aperture.

The radio source noise temperature increase measured by the antenna is given by [3]:

$$\Delta T = (\eta SA)/(2kC_rC_p)$$

where

- η = antenna aperture efficiency
- S = radio source flux, watts/m^2/Hz
- A = antenna area, m^2
- k = Boltzmann's constant, $1.38062 * 10^{-23}$ J/K (watt-second/kelvin)
- C_r = source size correction, typically 1.0 for point sources, up to ~1.5 for extended sources, including planets.
- C_p = pointing correction, assumed = 1.0

The flux, S, is typically given in units of "Janskys," where 1 Jansky (Jy) = 10^{-26} W/m^2/Hz.

Measured ΔT is compared with the quantity $[(SA)/(2kC_r)]$ to give antenna efficiency. Thus:

$$\eta = \Delta T/[(SA)/(2kC_r)]$$
$$= \Delta T/[\mathrm{T100}/C_r].$$

T100 is what would be measured by a perfect antenna looking at a point source emitting the same flux as the

TABLE I
RADIO SOURCES USED FOR *X*-BAND (8450-MHz) CALIBRATIONS @ f1 AND f3, SEPTEMBER 1990 AND NOVEMBER 1990

Source	Declination J2000.0	Peak Elev @ DSS 13 Lat = 35.25°	Flux, Jy	C_r	T100/C_r, K	Notes
3C274	12.391	67.1	44.555	1.087	13.477	(1)
3C123	29.671	84.4	9.404	1.0054	3.0753	(2)
DR21	42.329	82.9	19.902	1.0085	6.489	(2)
3C84	41.512	83.7	45.79	1.000	15.056	(3)
3C273	2.052	56.8	36.46	1.000	11.988	(3)

Notes
1) Ref. [5]
2) Ref. [6]
3) Ref. [7] values reduced by 0.076 dB as per Ref. [8] calibration analysis of 70-m antenna gain, and Ref. [9]

observed radio source. C_r is a function of the source structure at a particular frequency and the antenna pattern of a particular antenna at that frequency. For a particular antenna, frequency, and radio source, the T100/C_r can thus be specified.

For a planet, the flux is determined from the blackbody disk temperature and the angular size of the source (which changes as the distance between earth and the planet changes).

The flux is given by [4]:

$$S = (2kT\Omega)/(\lambda^2)$$

where

k = Boltzmann's constant
T = blackbody disk temperature, kelvins
λ = wavelength, meters
Ω = solid angle subtended by source = $(\pi D^2)/(4R^2)$
D = planet diameter, km
R = distance to planet, km

IV. CORRECTION FOR ATMOSPHERIC ATTENUATION

ΔT is an on-off source measurement, and the Earth's atmosphere attenuates the true source contribution that would be measured under vacuum conditions. The total atmospheric attenuation was estimated from surface weather conditions during all measurements. The surface temperature, pressure, and relative humidity at the site were recorded every half-hour. Typical zenith values of attenuation at Goldstone under average clear-sky conditions are:

$$X\text{-band: } A_{zen} = 0.035 \text{ dB}$$

$$Ka\text{-band: } A_{zen} = 0.115 \text{ dB}$$

The attenuation at an elevation angle θ is modeled as

$$A(\theta) = A_{zen}/\sin(\theta)$$

The loss factor at that elevation angle is

$$L(\theta) = 10^{A(\theta)/10}$$

The "vacuum ΔT" then becomes

$$\Delta T = L(\theta)\, \Delta T_{measured}$$

V. RADIO SOURCE FLUX VALUES AND SIZE CORRECTIONS

At both *X*- and *Ka*-bands, radio source 3C274 (Virgo A) is considered a principal calibrator, although at *Ka*-band Venus is considered well-enough known to be used as a primary source also. At both *X*- and *Ka*-bands, the principal calibrators are used to establish the peak antenna efficiency near the antenna rigging angle (40–50 degrees elevation). As these sources typically do not rise to high elevation angles, other sources which do are also used to establish the shape of the efficiency curve with elevation angle. High declination sources such as 3C84 and 3C123 are used for this purpose. As their fluxes are not well known (or the sources are variable) the efficiency curves so generated are normalized to the peak values determined by the principal calibrators.

Table I summarizes the flux, size correction, and other factors associated with the radio source calibrators used during the DSS-13 *X*-band calibration measurements. It should be noted that radio sources 3C84 and 3C273 are known to be variable; however they are point sources and are useful for pointing model development.

VI. EFFICIENCY MEASUREMENTS: *X*-BAND AT f1, SEPTEMBER 1990

Using the peak efficiency value determined by 3C274 to define the antenna performance, it was found that the efficiencies as determined by the other sources (using the T100/C_r values above) varied by as much as 40 percent. Adjustments were made to the data points of each source separately to normalize their curve-fitted peak values to the 3C274 curve-fitted peak value. Table II gives the required efficiency adjustments and the deduced flux and T100/C_r values thus obtained. In the case of point sources (3C84, 3C273), the adjustment reflects a flux error. For nonpoint or extended sources (DR21, 3C123) the adjustment could be due to either flux or source size correction

TABLE II
EFFICIENCY ADJUSTMENTS AND DEDUCED FLUX AND T100/C_r VALUES: X-BAND (8450 MHz) @ f1, SEPTEMBER 1990

Source	Efficiency Adjustment Needed	Deduced Flux, Jy	Deduced T100/C_r, K	Notes
3C274	1.00000	44.555	13.477	extended
3C123	0.98722	—	3.115	non-point
DR21	0.99478	—	6.523	non-point
3C84	1.40141	32.67	10.743	var, point
3C273	1.24420	29.30	9.635	var, point

errors (which are at present unable to be separated); thus only the deduced T100/C_r value is given. It should be noted that the variable sources (3C84, 3C273) may vary considerably over a period of weeks, thus the T100/C_r values found represent, at best, interim values.

The zenith atmosphere attenuation corrections made during these measurements ranged from 0.036 dB to 0.046 dB, during clear weather. The X-band peak efficiency of the DSS-13 antenna at f1 was determined to be 75.35 percent at an elevation angle of 45.63 degrees. This corresponds to a peak gain of 68.34 dBi at 8450 MHz.

The above efficiency value was measured in the "post-holography" condition of the antenna, with the main reflector panels in their final adjustment condition. After initial acceptance of the antenna in July 1990, preliminary X-band f1 efficiency measurements were made. These measurements yielded a peak efficiency of 71.88 percent. Thus the panel adjustment yielded an additional 3.5 efficiency-percent (a 0.21-dB improvement), in addition to resetting the rigging angle to near 45 degrees instead of the initial 58 degrees. (These values are shown in Table VIII, along with the results of all other post-holography measurements.) Fig. 2 shows the pre-/post-holography comparison. Fig. 3 shows the X-band f1 efficiency curve along with the adjusted data points.

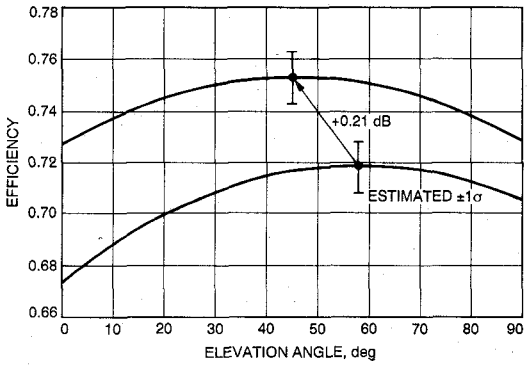

Fig. 2. DSS 13 X-band (8450-MHz) efficiency at f1, pre-holography (bottom) and post-holography (top), without atmosphere.

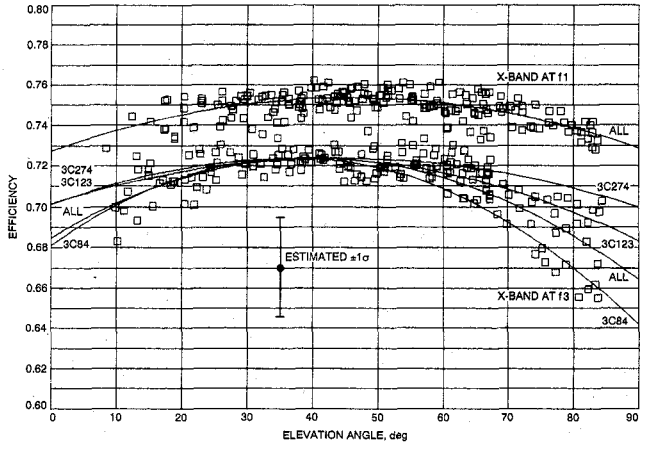

Fig. 3. DSS 13 X-band (8450-MHz) efficiency at f1 and f3 focal points, without atmosphere.

VII. EFFICIENCY MEASUREMENTS: X-BAND @ f3, NOVEMBER 1990

By methods similar to those described above, X-band f3 measurements were made two months later. The radio sources used were restricted to three: 3C274, 3C84, and 3C123. Atmospheric attenuation at zenith varied from 0.035 dB to 0.037 dB, a lower and smaller range than in September, undoubtedly due to lower water vapor contribution. Using 3C274 as the standard gain calibrator and the other two sources to provide shape information, it was found that the efficiency using the beam-waveguide system was somewhat lower than at f1. The final peak efficiency was determined to be 72.38 percent at an elevation angle of 40.21 degrees, a decrease of 2.97 percent. The corresponding f3 gain is 68.17 dBi. Table III gives the deduced flux and T100/C_r values determined using the f3 measurements.

It is seen that the T100/C_r value of 3C123 appears to have decreased 1.51 percent, and that of 3C84 appears to have decreased 2.12 percent in the two months between September and November 1990. Again, these changes are relative to 3C274, and because they are both small, may not be significant. As 3C123 is not considered to be variable, the 1.51 percent change may be due to noise in the data.

Fig. 3 shows the adjusted data points and individual curve fits for the three sources (3C123 and 3C84 adjusted). It appears that the fits for 3C123 and 3C84 are significantly different at high elevation angles (at meridian transit). Because of the different declinations of these two sources, 3C123 passes south at meridian transit and 3C84 passes north, although both are only 6 degrees from zenith. It is now believed that the different efficiency values at high elevation are azimuth-related, and are due to a misalignment of the ellipsoidal and flat mirrors at the

TABLE III
EFFICIENCY ADJUSTMENTS AND DEDUCED FLUX AND T100/C_r VALUES: *X*-BAND (8450 MHz) @ f3, NOVEMBER 1990

Source	Efficiency Adjustment Needed	Deduced Flux, Jy	Deduced T100/C_r, K	Notes
3C274	1.00000	44.555	13.477	extended
3C123	1.00240	—	3.068	non-point
3C84	1.43183	31.98	10.515	var, point

TABLE IV
RADIO SOURCES USED FOR *Ka*-BAND (32-GHz) CALIBRATIONS @ f1, OCTOBER 1990

Source	Declination J2000.0	Peak Elev @ DSS 13 Lat = 35.25°	Flux, Jy	C_r	T100/C_r, K	Notes
3C274	12.391	67.1	16.22	1.273	4.190	(1)
3C84	41.512	83.7	43.71	1.000	14.372	(2)
3C273	2.052	56.8	29.54	1.000	9.713	(2)
Venus 1990						
Oct 01	+1.6	1.69539 AU 56.4	27.323	1.00828	8.914	(3)
Oct 10	−2.9	1.70591 AU 51.9	26.987	1.00818	8.806	
Oct 20	−7.9	1.71302 AU 46.9	26.764	1.00811	8.733	
Oct 30	−12.5	1.71538 AU 42.3	26.690	1.00809	8.709	

Notes
1) Ref. [5]
2) Ref. [10]
3) Declination-of-date

TABLE V
EFFICIENCY ADJUSTMENTS AND DEDUCED FLUX AND T100/C_r VALUES: *Ka*-BAND (32 GHz) @ f1, OCTOBER 1990

Source	Efficiency Adjustment Needed	Deduced Flux, Jy	Deduced T100/C_r, K	Notes
3C274	0.98475	16.22	4.190	extended
Venus	1.01573	Table IV	Table IV	variable
3C84	1.49278	29.281	9.628	var, point
3C273	0.94022	31.418	10.331	var, point

bottom of the beam-waveguide system. At meridian transit, these two sources have 180 degree different azimuths. Note that 3C274, which also passes south of the antenna at meridian transit (although at only 67 degrees elevation), has a curve fit more like that of 3C123, which also passes south.

VIII. EFFICIENCY MEASUREMENTS: *Ka*-BAND @ f1, OCTOBER 1990

The four radio sources used for *Ka*-band measurements were 3C274, 3C84, 3C273, and Venus. The 3C274 flux appears to be well known, as determined in a recent analysis at JPL [5]. The source size correction was calculated by integrating the antenna beam (0.017-degree beamwidth) over a frequency-extrapolated map of the source. The source-size correction thus determined was 1.273. The flux of 3C84 was unknown, but a starting value was used based on 32-GHz measurements carried out on the Goldstone 70-meter antenna (DSS 14) in 1989 [10]. In that report, a flux of 43.71 Janskys was deduced with reference to measurements made using 3C274 and Venus as standard calibrators. It was found during the f1 measurements that this value required substantial adjustment to

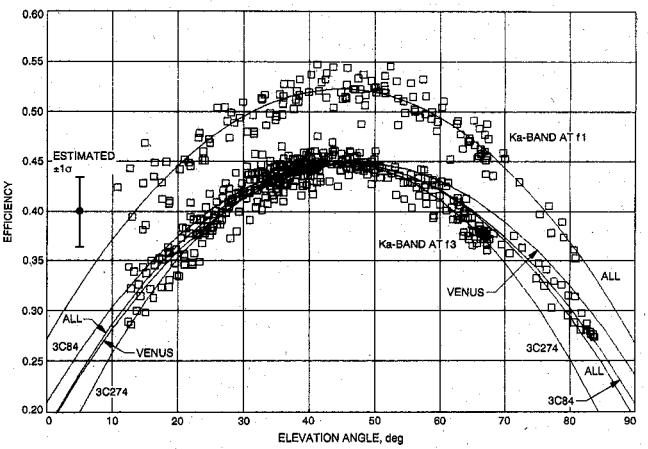

Fig. 4. DSS 13 *Ka*-band (32-GHz) efficiency at f1 and f3 focal points, without atmosphere.

TABLE VI
RADIO SOURCES USED FOR *Ka*-BAND (32-GHz) CALIBRATIONS @ f3, JANUARY 1991

Source	Declination J2000.0	Peak Elev @ DSS 13 Lat = 35.25°	Flux, Jy	C_r	T100/C_r, K	Notes
3C274	12.391	67.1	16.22	1.273	4.190	(1)
3C84	41.512	83.7	—	1.000	10.000	(2) (3)
Venus 1991						
Jan 01	−22.5	1.63496 AU 32.3	29.380	1.00891	9.579	(4)
Jan 10	−20.2	1.61115 AU 34.6	30.255	1.00918	9.862	
Jan 20	−16.8	1.58115 AU 38.0	31.414	1.00953	10.236	
Jan 30	−12.6	1.54728 AU 42.2	32.804	1.00995	10.685	

Notes
1) Ref. [5]
2) Ref. [10]
3) Dummy value for T100/C_r, based on 9.628 found at f1
4) Declination-of-date

bring the October 1990 efficiency measurements into agreement with those determined by Venus and 3C274.

Flux from Venus was calculated from the expression given above in Section III. The source size correction, C_r, for a disk is calculated from [11]:

$$C_r = X/(1 - e^{-x})$$

where

$X = (r^2)/(2\sigma^2)$
r = angular radius of disk, degrees
$\sigma = \Theta_o/2.3548$, degrees
Θ_o = full 3-dB antenna bandwidth, degrees

T100/C_r is calculated as usual from

$$\text{T100}/C_r = (SA)/(2kC_r)$$

as described above.

A value of 475 kelvins was used for the blackbody disk temperature of Venus [10 and 12]. The planetary disk diameter of Venus used was 12240 km [12]. During the *Ka*-band f1 measurement period, Venus was near superior conjunction, and the distance from Earth to Venus changed very little, from about 1.70 to 1.72 AU. Table IV gives the values used in the *Ka*-band calibration at f1.

Using the above T100/C_r values for the sources listed, the f1 efficiency as determined using Venus was found to be 51.50 percent. Using 3C274, the efficiency was found to be 53.12 percent. As both sources are regarded to be standard calibrators, the results were averaged, yielding a final f1 efficiency value of 52.31 percent at an elevation angle of 44.82 degrees. The corresponding gain is 78.33 dBi. The zenith atmospheric attenuation during the measurement period ranged from 0.133 dB to 0.233 dB. Adjustments in the flux and T100/C_r values of 3C84 and 3C273 were made in order to match the efficiency found above. Table V gives these adjustments.

It should be noted that the adjustments shown for 3C274 and Venus are shown as needed only to establish an average peak gain value. As the sources are considered to be standard calibrators, the adjustments do not imply new flux or T100/C_r values.

TABLE VII
EFFICIENCY ADJUSTMENTS AND DEDUCED FLUX AND T100/C_r VALUES: *Ka*-BAND (32 GHz) @ f3, JANUARY 1991

Source	Efficiency Adjustment Needed	Deduced Flux, Jy	Deduced T100/C_r, K	Notes
3C274	1.03417	16.22	4.190	extended
Venus	0.96804	Table VI	Table VI	variable
3C84	1.02592	29.643	9.747	var, point

Fig. 4 shows the adjusted data points and the curve fit for the *Ka*-band f1 measurements.

IX. EFFICIENCY MEASUREMENTS: *Ka*-BAND @ f3, JANUARY 1991

Ka-band measurements at f3 during December 1990 showed a very apparent efficiency anomaly which unfortunately became known as the "hysteresis effect," because it was initially thought to be due to a mechanical inelasticity (which turned out not to be the case). After numerous tests, it was determined that the most likely cause of this effect was a misalignment of the ellipsoidal mirror in the pedestal room. Realignment of the mirror was done in early January 1991. It was then decided to re-do the *Ka*-band f3 measurements throughout that month. Only Venus, 3C274, 3C84 were used for these tests. Table VI gives the flux and T100/C_r values used during the *Ka*-Band f3 measurements. Note that a dummy value of T100/C_r = 10.000 is used for 3C84 (based on 9.629 deduced at f1). The real value would be determined after comparison with the Venus and 3C274 efficiency results.

Zenith atmospheric attenuation during these tests varied from 0.096 dB to 0.120 dB, substantially lower than during the f1 tests. Weather during the tests was clear and very cold, with very low absolute humidity. Table VII gives the efficiency adjustments needed and the deduced values of flux and T100/C_r. Note that although adjustments are shown for Venus and 3C274, the given values of flux and T100/C_r are not changed from the initial val-

TABLE VIII
DSS 13 BWG ANTENNA *X*- AND *Ka*-BAND FINAL PEAK GAINS AND EFFICIENCIES

	X-Band (8450 MHz)		*Ka*-Band (32 GHz)	
	Gain (dBi)	Efficiency	Gain (dBi)	Efficiency
f1 pre-holography	68.14	71.88%	—NA—	
	@ 58.03° elevation			
f1 post-holography	68.34	75.35%	78.33	52.31%
	@ 45.63° elevation		@ 44.82° elevation	
f3 post-holography	68.17	72.38%	77.66	44.89%
	@ 40.21° elevation		@ 45.41° elevation	

Estimated $1-\sigma$ Errors:
X-Band: 2.3 efficiency-percent 0.14 gain-dB
Ka-Band: 3.6 efficiency-percent 0.33 gain-dB

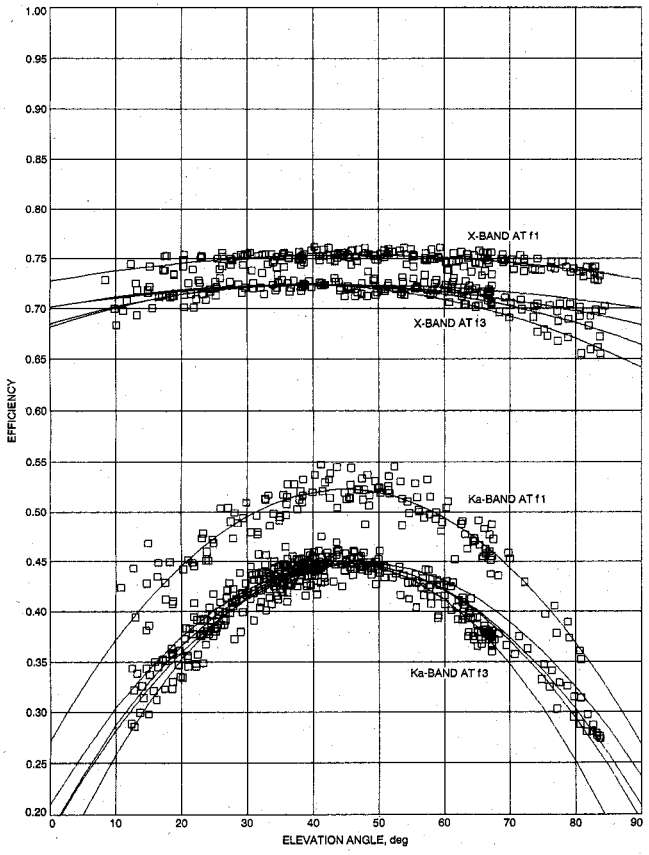

Fig. 5. DSS 13 *X*- and *Ka*-band efficiencies at f1 and f3 focal points, without atmosphere.

ues given above, as they are considered to be calibration standards.

The peak *Ka*-band f3 efficiency was determined to be 44.89 percent at an elevation angle of 45.41 degrees. This corresponds to a gain of 77.66 dBi.

Several things should be noted about Table VII: 1) Compared with the *Ka*-band f1 measurements, the 3C274 and Venus adjustment directions have been reversed; 2) The adjustment for 3C84 is based on an assumed $T100/C_r$ value of 10.000, a dummy value; 3) The final deduced flux and $T100/C_r$ values for 3C84 vary only by 1.24 percent from those determined in the f1 measurements, even though the source is variable and three months time had elapsed. This may hint at the period of variation of the source.

TABLE IX
COEFFICIENTS OF POLYNOMIALS FOR DSS 13 BWG ANTENNA *X*- AND *Ka*-BAND EFFICIENCIES WITHOUT ATMOSPHERE

Efficiency (w/o atm) $= a_0 + a_1 * \theta + a_2 * \theta^2$ where θ = antenna elevation angle, degrees

	a_0	a_1	a_2
X-Band @ f1	0.72734	0.00114701	−0.0000125694
X-Band @ f3	0.68496	0.00192912	−0.0000239880
Ka-Band @ f1	0.27220	0.01119613	−0.0001249108
Ka-Band @ f3	0.18285	0.01171770	−0.0001290241

Fig. 4 shows the adjusted data points and the curve fits for the three calibration sources. Again, the spread of curve fits at the high elevation angles shows the effect of possible ellipsoidal mirror misalignment. Note that the mirror alignment for the *Ka*-band f3 tests is different than that for the *X*-band f3 tests in November 1990. Compared with the *X*-band curve fits, the southern-passing sources (3C274, Venus) straddle the curve fit of the northern-passing source (3C84), rather than being above it. Because of the low declination of Venus during the f3 tests (resulting in low peak elevation angle), the curve fit at high elevation angles may be in error, thus giving this result.

X. FINAL RESULTS

Table VIII gives a summary of the final gain and efficiency measurements described above. In addition, the estimated 1-σ errors are given, as well as shown on Figs. 3 and 4. The errors are due to source flux uncertainty, source size correction error, and data noise, curve fitting, and data reduction methodology. For purposes of comparison, Fig. 5 shows all data sets and curve fits together. The frequency-dependent effect of main-reflector structural deformation is seen in this figure.

Table IX gives the coefficients of the final antenna ef-

TABLE X
FINAL RADIO SOURCE FLUX AND T100/C_r VALUES DEDUCED FROM DSS 13 34-m ANTENNA EFFICIENCY MEASUREMENTS

Frequency	Source	Flux, Jy	C_r	T100/C_r	Notes
8450 MHz	3C274	44.555	1.087	13.477	(1) (2)
X-Band	3C123	—	—	3.092	(2)
	DR21	—	—	6.523	(3)
	3C84	32.67	1.000	10.629	(2) (4)
	3C273	29.30	1.000	9.635	(3) (4)
32 GHz	3C274	16.22	1.273	4.190	(1) (2)
Ka-Band	3C84	29.462	1.000	9.688	(2) (4)
	3C273	31.418	1.000	10.331	(3)
	Venus		—see text—		(1) (2) (4)

Notes
1) Calibration standard, no new values deduced
2) f1 and f3 measurements
3) f1 measurement only
4) Variable source

ficiency curve-fit polynomials used in the generation of Figs. 3, 4, and 5.

Table X gives final radio source flux and T100/C_r values deduced from the efficiency measurements described above. When two different values have been found from f1 and f3 measurements, the value presented here is the average of the two. These values are, at least, a starting point for future measurements. In the case of standard calibrators (3C274, Venus), no new values are given. The T100/C_r values given for non-point sources are valid only for use in the calibration of 34-meter-diameter antennas with *X*- and *Ka*-band beamwidths of 65 and 17 mdeg, respectively. The C_r values were calculated using these beamwidths. Care should be taken in calibration measurements when the antenna beamwidth varies from these numbers. Simple modeling is typically not accurate.

XI. CONCLUSION

This article has presented a complete review of the initial 8.45- and 32-GHz efficiency calibration of the new NASA Deep Space Network beam-waveguide antenna at the Goldstone Deep Space Communications Complex. The novel technique of using portable test packages to evaluate antenna performance at various locations in the microwave optics path has proved to be straightforward to implement and successful in operation. At the beam-waveguide focus, 8.45- and 32-GHz peak efficiencies of 72.38 and 44.89 percent, respectively, were achieved. The efficiency determinations presented here met the functional requirements of the DSS 13 project and agreed well with predictions which considered feed illumination and spillover, waveguide and mirror losses, and beam-waveguide effects.

ACKNOWLEDGMENT

The authors wish to thank R. L. Riggs for the development of the boresight methodology and programming, without which the measurements described here would have been impossible. P. H. Richter provided updated radio source flux and source size correction values. We are also indebted to the Goldstone DSS 13 personnel who supported us during the many months of the measurement program.

REFERENCES

[1] D. A. Bathker, W. Veruttipong, T. Y. Otoshi, and P. W. Cramer, Jr., "Beam-waveguide antenna performance predictions with comparisons to experimental results," *Microwave Theory Tech.*, vol. 40, no. 6, June 1992.
[2] T. Y. Otoshi, S. R. Stewart, and M. M. Franco, "Portable microwave test packages for beam-waveguide antenna performance evaluations," *Microwave Theory Tech.*, vol. 40, no. 6, June 1992.
[3] J. A. Turegano and M. J. Klein, "Calibration radio sources for radio astronomy: Precision flux density measurements at 8420 MHz," *Astron. Astrophys.*, vol. 86, pp. 46–49, 1980.
[4] ——, "Precision flux density measurements of the giant planets at 8420 MHz," *Astron. Astrophys.*, vol. 94, pp. 91–94, 1981.
[5] P. H. Richter, "Virgo-A flux density," JPL IOM 3393-90-137, Internal Document, Oct. 18, 1990.
[6] ——, personal communication, Jet Propulsion Laboratory, July 26, 1990.
[7] M. Klein *et al*, "DSN radio source list for antenna calibration," *JPL Document D-3801, Rev. B*, Internal Document, Sept. 25, 1987.
[8] P. H. Richter and S. D. Slobin, "DSN 70-meter antenna X- and S-band calibration, Pt. I: Gain measurements," *JPL TDA Progress Report 42-97*, p. 319, June 15, 1989.
[9] P. H. Richter and S. D. Slobin, "errata to Reference 6 article," *JPL TDA Progress Report 42-99*, p. 220, Nov. 15, 1989.
[10] M. S. Gatti, M. J. Klein, and T. B. H. Kuiper, "32-GHz performance of the DSS-14 70-meter antenna; 1989 configuration," *JPL TDA Progress Report 42-99*, pp. 206–219, Nov. 15, 1989.
[11] P. H. Richter, personal communication, Jet Propulsion Laboratory, Oct. 1, 1990.
[12] P. G. Steffes, M. J. Klein, and J. M. Jenkins, "Observations of the microwave emission of Venus from 1.3 to 3.6 cm," *Icarus*, vol. 84, pp. 83–92, 1990.

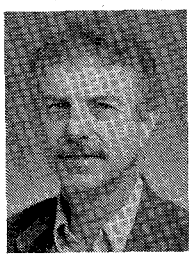

Stephen D Slobin was born in Los Angeles, CA, on January 18, 1941. He received the B.S. degree in engineering from the California Institute of Technology in 1961, and the M.S. and Ph.D. degrees in electrical engineering from the University of Southern California in 1963 and 1969.

From 1969 to 1970 he was with TRW Systems Group, Redondo Beach, CA, where he worked in the area of remote sensing. From 1972 to 1974 he was with Aerojet Electrosystems Company, Azusa, CA, where he carried out antenna analysis and radar meteorology studies. Since 1975 he has been with the Jet Propulsion Laboratory, Pasadena, CA, where he has been involved in gain and noise temperature calibrations of the NASA Deep Space Network antennas and has developed weather effects models for use in telecommunications link design.

Tom Y. Otoshi (S'53–M'56–SM'74), for photograph and biography, see this issue, p. 1292.

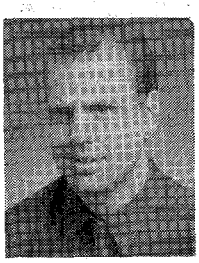

Mike Britcliffe received the B.S. degree in applied physics from California State University, Northridge.

He has been involved with JPL and the NASA Deep Space Network for 16 years working in areas including antenna system integration and test, high power transmitter development and the implementation of cryogenically cooled low-noise amplifiers. He is currently responsible for antenna metrology engineering in the ground antenna and facilities engineering section at the Jet Propulsion Laboratory.

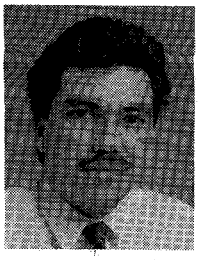

Leon S. Alvarez, (M'88) received the B.Sc. degree in mechanical engineering from the University of California, San Diego in 1986 and the S.M. degree in electrical engineering from the Massachusetts Institute of Technology in 1988.

He has been with the Jet Propulsion Laboratory since 1987 where he has worked in the areas antenna axis servo control system modeling and design and calibration methods for precision pointing of large structure antennas. His interests include linear regression, application of classical control theory and modern control and estimation theory, and large scale system design, simulation and analysis.

Scott R. Stewart, (S'87–M'89), for photograph and biography, see this issue, p. 1293.

Manuel M. Franco (M'91), for photograph and biography, see this issue, p. 1293.